Periodic-Orbit Bifurcation and Shell Structure in Reflection-Asymmetric Deformed Cavity

Ayumu Sugita,[a] Ken-ichiro Arita[b] and Kenichi Matsuyanagi[a]

[a] *Department of Physics, Graduate School of Science, Kyoto University, Kyoto 606-01, Japan*

[b] *Department of Physics, Nagoya Institute of Technology, Nagoya 466, Japan*

Abstract

Shell structure of the single-particle spectrum for reflection-asymmetric deformed cavity is investigated. Remarkable shell structure emerges for certain combinations of quadrupole and octupole deformations. Semiclassical periodic-orbit analysis indicates that bifurcation of equatorial orbits plays an important role in the formation of this new shell structure.

Theoretical and experimental exploration of reflection-asymmetric deformed shapes is one of the current topics of interest both in nuclear-structure and micro-cluster physics[1,2,3,4].

In theoretical calculations, various approaches like Hartree-Fock-Bogoliubov methods, microscopic-macroscopic methods and semi-classical methods have been exploited for this aim (see Ref. [1] for a review). Each method possesses merits and demerits, so that it would be desirable to explore the subject with various approaches.

A basic motive of the semi-classical periodic-orbit approach[5,6,7] is to understand the origin of shell-structure formation that play decisive role in bringing about symmetry-breaking in the average potential of finite quantum systems like nuclei and micro-cluster. If we could understand the origin and obtain a global perspective, it would become possible to qualitatively predict where we can expect a particular deformation to appear in the multi-dimensional space spanned by various deformation-parameters and the number of constituents of the system.

In the conventional wisdom, shell-structure would be weakened if reflection-asymmetric deformation is added to the spheroidal shape. This is because the system becomes non-integrable when the octupole deformation is added, and because the degeneracy of the periodic-orbits is then reduced. Contrary to this expectation, a significant shell structure was found in Refs. [8,9] to emerge for certain combinations of quadrupole and octupole deformations in the reflection-asymmetric deformed oscillator model. It was pointed out that this shell-structure enhancement is associated with bifurcation of periodic orbits.

It would be very important to investigate whether such a mechanism of shell-structure formation is special to the harmonic-oscillator model or possesses more general significance.

To explore the possibility that significant shell structure emerges in the single-particle spectra for non-integrable Hamiltonian, we have carried out an analysis of single-particle motions in the reflection-asymmetric, axially-symmetric deformed cavity by parameterizing the surface as

$$R(\theta) = R_0 \left(\frac{1}{\sqrt{(\frac{\cos\theta}{a})^2 + (\frac{\sin\theta}{b})^2}} + a_3 Y_{30}(\theta) \right), \quad (1)$$

where a and b are related with the familiar quadrupole deformation parameter δ (equivalent to δ_{osc} in Ref. [10]) by $a = ((3+\delta)/(3-2\delta))^{2/3}$ and $b = ((3-2\delta)/(3+\delta))^{1/3}$. It reduces to spheroid (integrable cavity) in the limit that the octupole deformation parameter a_3 vanishes.

We solve the Schrödinger equation under the Dirichlet boundary condition and evaluate the shell energy by means of the Strutinsky method. To effectively obtain a large numbers of eigenvalues as a function of deformation parameters, we have examined four numerical recipes; the plane-wave decomposition (PWD)[11], the spherical-wave decomposition (SWD)[12], the boundary integral method (BIM)[13,14,15] and the coordinate-transformation method (DIAG)[16,17]. The DIAG is the most effective method for near-spherical shape, but not good for strongly deformed shape. In SWD, PWD and BIM, eigenvalue problem is converted to a search of the zeros of real function, minima of positive function and zeros of complex function, respectively, and we found SWD is most convenient for the present purpose. Thus we mainly use this method, sometimes cross-checking the results by other methods.

Figure 1 shows a typical example of the single-particle spectrum calculated as a function of the octupole-deformation parameter a_3 fixing the quadrupole-deformation parameter at $\delta = 0.3$. It is seen that a new shell structure emerges at about $a_3 = 0.2$. Deformed magic numbers associated with this shell structure are 26,42,70,114,172,..., taking the spin degeneracy factor into account. Note that these numbers appear at intermediate places between the magic numbers 20,58,92,138,186,... of the spherical cavity. This indicates that, due to the reflection-symmetry breaking of the cavity, strong $\Delta l = 3$ mixing takes place among levels with large orbital angular momenta l in spherical major shells.

Figure 2 shows shell-structure energies evaluated with the standard Strutinsky procedure and plotted as functions of the particle number N. As expected from Fig. 1, we confirm here that minima develop in association with the formation of the new shell structure at about $a_3 = 0.2$.

To understand the physical reason why such a remarkable shell structure emerge for a certain combination of the octupole and quadrupole deformations, and to identify the classical periodic orbits
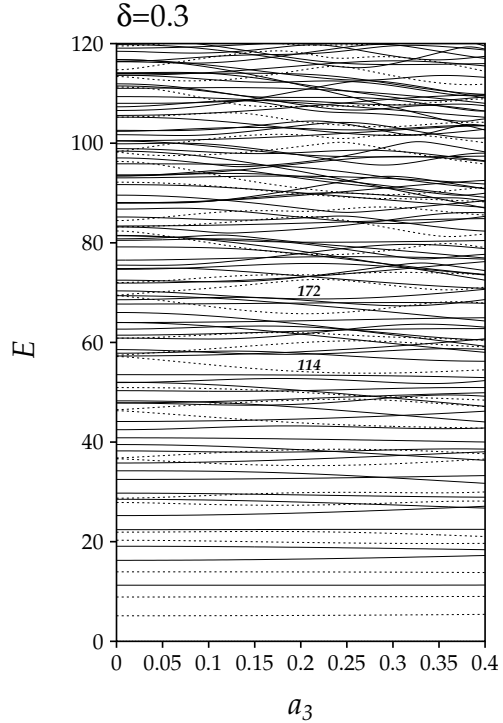

Fig. 1. Single-particle-energy spectrum of the deformed cavity plotted as a function of the octupole deformation parameter a_3. The quadrupole deformation parameter is fixed at $\delta = 0.3$. The energy is measured in unit of $\hbar^2/MR_0^2$, M being the mass.
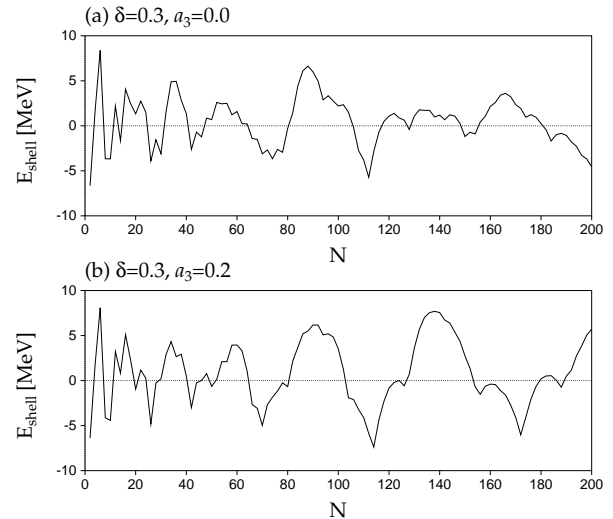

Fig. 2. Shell structure energies of the deformed cavities with $\delta = 0.3$ and $a_3 = 0.0$(a), 0.2(b), evaluated with the conventional Strutinsky method and plotted as functions of the particle number N. The energy is evaluated by putting $R_0 = 1.2(2N)^{1/3}$fm and $Mc^2 = 938$MeV, for nuclei.

responsible for this shell structure formation, we analyze Fourier transform of the quantum spectrum.

The single-particle equations of motion for the cavity are invariant with respect to the scaling transformation $(\boldsymbol{x}, \boldsymbol{p}, t) \to (\boldsymbol{x}, \alpha \boldsymbol{p}, \alpha^{-1} t)$. The action integral S_γ for the periodic orbit γ corresponds to the length L_γ of it,

$$S_\gamma(E = p^2/2M) = \oint_\gamma \boldsymbol{p} \cdot d\boldsymbol{q} = p L_\gamma, \qquad (2)$$

and the Gutzwiller trace formula is written as

$$\rho(E) \simeq \bar{\rho}(E) + \sum_\gamma A_\gamma k^{(d_\gamma - 2)/2} \cos(k L_\gamma - \pi \mu_\gamma/2), \qquad (3)$$

where $\bar{\rho}(E)$ denotes the contributions of orbits of 'zero- length', d_γ the degeneracy and μ_γ the Maslov phase of the periodic orbit γ. This scaling property enables us to make use of the Fourier transformation of the level density with respect to the wave number k. The Fourier transform $F(L)$ of the level density $\rho(E)$ is written as

$$F(L) = \int dk \, k^{-(d-2)/2} e^{-ikL} \rho(E = \hbar^2 k^2/2M)$$
$$\simeq \bar{F}(L) + \sum_\gamma A'_\gamma \delta(L - L_\gamma). \qquad (4)$$

which may be regarded as 'length spectrum' exhibiting peaks at the lengths of individual periodic orbits. In numerical calculation, the spectrum is cut off by Gaussian with cut-off wave number $k_c = 1/\Delta L$ as

$$F_{\Delta L}(L) \equiv \int dk \, k^{-(d-2)/2} e^{-ikL} e^{-\frac{1}{2}(k/k_c)^2}$$
$$\times \rho(E = \hbar^2 k^2/2M)$$
$$= \frac{M}{\hbar^2} \sum_n k_n^{-d/2} e^{-ik_n L} e^{-\frac{1}{2}(k_n/k_c)^2} \qquad (5)$$
$$\simeq \bar{F}_{\Delta L}(L) + \sum_\gamma A''_\gamma \exp\left[-\frac{1}{2}\left(\frac{L - L_\gamma}{\Delta L}\right)^2\right]. \qquad (6)$$

The amplitude A_γ (or A''_γ) is proportional to the stability factor $1/\sqrt{|2 - \operatorname{Tr} M_\gamma|}$ (in stationary-phase
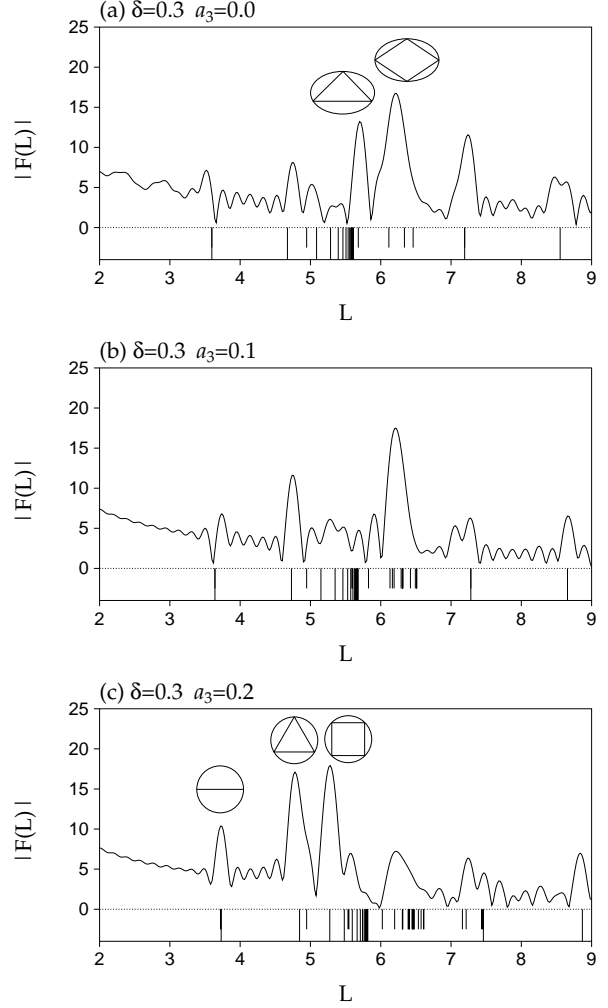

Fig. 3. Fourier transforms of the quantum level densities for the deformed cavities with $\delta = 0.3$ and $a_3 = 0.0$(a), 0.1(b), 0.2(c). The degeneracy index $d = 1$ (valid for generic periodic orbits) and Gaussian cut-off wave number $k_c = \sqrt{300}$ are used in (5). In each panel, lengths of classical periodic orbits in the axis-of-symmetry (equatorial) plane are indicated by short (long) vertical lines. The lengths are measured in unit of the radius R_0.

approximation), where M_γ is the monodromy matrix of orbit γ, and expected to be enhanced in the vicinity of the bifurcation point where $\operatorname{Tr} M_\gamma = 2$ (see Ref. [9]).

Let us investigate how these peaks change when the shape parameters of the cavity is varied. Figure 3 shows, as an example, how the pattern of the Fourier transform (5) changes as a function of a_3, fixing the quadrupole deformation parameter at $\delta = 0.3$. The highest peaks at the spheroidal limit ($a_3 = 0$) are associated with triangular and quadrilateral orbits
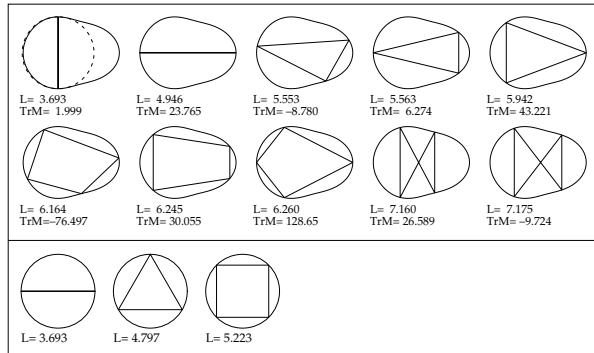
Fig. 4. Periodic orbits in the deformed cavity with $\delta = 0.3$ and $a_3 \simeq 0.16$ (at bifurcation). For each periodic orbit, the length L and the trace of the monodromy matrix, Tr M, are indicated. Those in the axis-of-symmetry plane are displayed in the upper panel and those in the equatorial plane in the lower panel. Only linear, triangular and quadrilateral orbits are displayed. In the top-leftmost figure, a sphere tangent to the boundary at equatorial plane is indicated by a broken line.
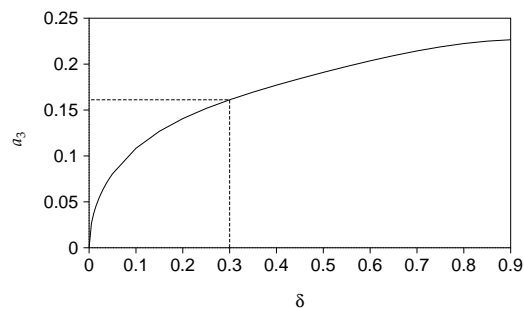

Fig. 5. Bifurcation line of the equatorial periodic orbits in the quadrupole-octupole deformation parameter space. For $\delta = 0.3$, bifurcation occurs at $a_3 \simeq 0.16$.

in the axis-of-symmetry plane, whose degeneracies are two. It is clearly seen that these peaks decline with increasing a_3. This is because the octupole deformation breaks the spheroidal symmetry and the degeneracy reduces to one corresponding to the rotation about the symmetry axis. On the other hand, we can clearly see that new peaks rise with increasing a_3. These new peaks are found to be associated with the periodic orbits in the equatorial plane at the center of the larger cluster of the pear-shaped cavity.

The key to understand the reason why such equatorial orbits start to play increasingly important roles at finite octupole deformation may lie in the following point: At certain combinations of δ and a_3, the curvature radius of the cluster matches with its radius, as illustrated in Fig. 4. This means that

the phase space structure around these periodic orbits *locally* becomes that of 'spherical' one. Then bifurcation of these equatorial periodic orbits occurs and new three-dimensional orbits are born. Figure 5 shows the bifurcation lines of this kind in the quadrupole-octupole deformation parameter space. The bifurcation occurs at $a_3 \simeq 0.16$ for the case $\delta = 0.3$. In general, remarkable shell structure may appear along the bifurcation line and stabilizes the reflection-asymmetric deformed shapes.

In conclusion, we have investigated shell structure of the single-particle spectrum in reflection-asymmetric deformed cavity. It is found that remarkable shell structure emerges for certain combinations of quadrupole and octupole deformations. Semiclassical periodic-orbit analysis has been carried out, and it is found that bifurcation of periodic orbits in the equatorial plane plays an important role in the formation of this new shell structure.

A more detailed analysis of the equatorial-orbit bifurcation will be reported elsewhere.

Acknowledgments

References

[1] S. Åberg, H. Flocard and W. Nazarewicz, Ann. Rev. Nucl. Part. Sci. 40 (1990) 439.

[2] P.A. Butler and W. Nazarewicz, Rev. Mod. Phys. 68 (1996) 349.

[3] M. Brack, S. Creagh, P. Meier, S. Reimann and M. Seidl, to be published in Proc. of the NATO ASI *Large Clusters of Atoms and Molecules*, Erice 1995, edited by T.P. Martin.

[4] W.D. Heiss, R.G. Nazmitdinov and S. Radu, Phys. Rev. B 51 (1995-I) 1874.

[5] M.C. Gutzwiller, J. Math. Phys. 12 (1971) 343.

[6] R. Balian and C. Bloch, Ann. Phys. 69 (1972) 76.

[7] V.M. Strutinsky, A.G. Magner, S.R. Ofengenden and T. Døssing, Z. Phys. A 283 (1977) 269.

[8] K. Arita, Phys. Lett. B 335 (1994) 279.

[9] K. Arita and K. Matsuyanagi, Nucl. Phys. A 592 (1995) 9.

[10] A. Bohr and B.R. Mottelson, *Nuclear Structure* (Benjamin, 1975) Vol. 2.

[11] E.J. Heller, in *Chaos and quantum systems, Proc. NATO ASI Les Houches Summer School*, 1991, edited by M-J. Giannoni, A. Voros and J Zinn-Justin (North-Holland) p.547.

[12] T. Mukhopadhyay and S. Pal, Nucl. Phys. A 592 (1995) 291.

[13] M.V. Berry and M. Robnik, J. Phys. A: Math. Gen. 19 (1986) 649.

[14] M.V. Berry and M. Wilkinson, Proc. R. Soc. Lond. A 392 (1984) 15.

[15] B. Li and M. Robnik, J. Phys. A: Math. Gen. 27 (1994) 5509.

[16] S.A. Moszkowski, Phys. Rev. 99 (1955) 803.

[17] J. Blocki, J. Skalski and W.J. Swiatecki, Nucl. Phys. A 594 (1995) 137.